

# Time dependence of forces between mica surfaces in water and its relation to the release of surface ions

Uri Raviv and Pierre Laurat<sup>a)</sup>

Weizmann Institute of Science, Rehovot 76100, Israel

Jacob Klein<sup>b)</sup>

Weizmann Institute of Science, Rehovot 76100, Israel and Physical and Theoretical Chemistry Laboratory, South Parks Road, Oxford OX1 3QZ, United Kingdom

(Received 5 September 2001; accepted 11 December 2001)

A surface force balance has been used to investigate the time-dependent behavior of the normal forces between two smooth mica surfaces immersed in salt-free (conductivity) water. A long-ranged repulsion on initial approach to adhesive contact indicates an equilibrium surface-charge density  $\sigma = \sigma_0$  due to the loss of  $K^+$  ions from the mica surface into the water. Subsequent force measurements at times  $\tau$  following separation of the surfaces reveal that  $\sigma$  drops markedly following contact and separation, but then relaxes back to  $\sigma_0$  with a characteristic time  $\tau_r = 11 \pm 2$  min. This behavior is attributed to condensation of the counterions into the surfaces when they come into contact, and to their subsequent slow release into the water. The energy barrier associated with the counterion release was estimated from the value of  $\tau_r$  to be  $33 \pm 4 k_B T$ . © 2002 American Institute of Physics. [DOI: 10.1063/1.1447911]

## INTRODUCTION

The properties of water in the vicinity of surfaces and under confinement have been studied extensively because of their importance not only in colloidal dispersions and in tribology, but also because of their relevance to a quantitative understanding of many processes in biological systems. These properties influence the rates and effectiveness of processes such as the transport of materials and energy in the cell, enzymatic activity of proteins, biochemical reactions, interactions between biomacromolecules, and the function of membranes. They are also important in technological problems including oil recovery from natural reservoirs, mining, catalysis, and corrosion inhibition. Water is found in high surface-to-volume geometries in porous materials such as Vycor glass, silica gel, and zeolites as well as in polymer gels, clays, rocks, sandstones, micelles, vesicles, and micro-emulsions.<sup>1–9</sup> Thin films of water between clay mineral surfaces and particles are responsible for their swelling or shrinking. Hysteresis of water content–suction relationships in clays were noted in early studies of the swelling properties of clays.<sup>10</sup> The ion exchange process in natural aluminosilicates such as muscovite mica have been studied as well<sup>11,12</sup> and found to be strongly related to the hydration forces of the exchanged ions, and may take hours to be completed.

The surface force balance (SFB) technique has been used to probe the properties of ultrathin aqueous films confined between two molecularly smooth mica surfaces. Normal forces between two curved mica surfaces immersed in water have previously been measured as a function of the separation between the surfaces.<sup>13–16</sup> Long-range repulsive

double layer forces measured between purified water with no added salt (conductivity water) have been attributed to potassium ( $K^+$ ) ions that dissolve from the mica surface into the solution, to dissolved  $CO_2$  from air, to hydroxonium ions (essentially hydrated protons,  $H_3O^+$ ), and to ions leached from glassware.<sup>15</sup> In conductivity water, most of the potassium ions on the mica surfaces are exchanged with  $H_3O^+$  ions<sup>15</sup> and the additional short-ranged repulsive hydration forces which dominate the interactions at higher salt concentrations<sup>15,17–19</sup> are not observed. As a result, at close separations the van der Waals (vdW) attraction overcomes the relatively weak repulsion between the surfaces, causing a jump into a strongly adhesive contact, at which point the protons (from the  $H_3O^+$  ions) condense into the surfaces to neutralize the surface charges. The general assumption in all these studies has been that the forces are in equilibrium and are reversible.<sup>20</sup>

In this study we examine the magnitude of the normal forces between mica surfaces interacting across conductivity water as a function of the time elapsed (equilibration time) subsequent to their separation from adhesive contact. We find a striking change both in the long- and short-ranged interactions between the surfaces as this time increases, and a relaxation to the limiting long-time behavior is observed. We attribute this to a condensation of counterions into the mica surface when they come into contact, and their subsequent slow release—over an associated energy barrier—into the water.

## EXPERIMENT

The normal forces  $F(D)$  between two opposing curved mica surfaces (of mean radius  $R$ ) as a function of their closest separation  $D$ , was directly measured using a SFB (see inset of Fig. 1), for which detailed experimental procedures

<sup>a)</sup>Current address: Service Recherche Technologies Systems, LEGRAND SA 128, avenue de Latte de Tassigny, 87045, Limoges Cedex, France.

<sup>b)</sup>Author to whom correspondence should be addressed.

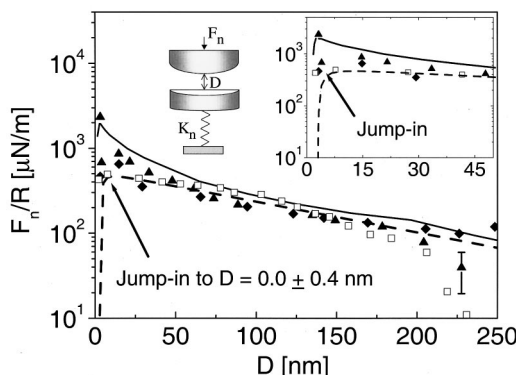


FIG. 1. Force–distance profiles between curved mica surfaces in conductivity water ( $pH=6.0\text{--}6.2$ ), where the force axis is normalized as  $F/R$  ( $R$ —mean radius of curvature of the mica surfaces  $\sim 1$  cm), taken on a first approach after introduction of the conductivity water into the cell and equilibration for 2 h or more. Different symbols indicate different sets of experiments, with all measurements being taken during compression. The open squares are from an approach run taken 69 min subsequent to separation from contact. From  $D_j=3.5\pm 1$  nm, there were jump-ins to flat adhesive contact. Note that in air a water-soluble layer [probably water and  $\text{CO}_2$  (Ref. 32)] adsorbs on the exposed mica surface in air (Refs. 13 and 33) and, when the surfaces are immersed in conductivity water, this layer is also squeezed out, resulting in a jump-in to  $D=-0.5\pm 0.3$  nm (average of four experiments) with respect to the air contact position. This separation in conductivity water represents the mica/mica contact, and is defined as  $D=D_0=0.0\pm 0.4$  nm; all  $D$  values are then given with respect to  $D_0$ . The solid line corresponds to the results of earlier studies performed by Pashley (Ref. 15). The dashed line is the best fit of the linear parts of the profiles to the DLVO expression, Eq. (1). From the fit to our data we obtained  $\kappa^{-1}=120\pm 20$  nm, corresponding to  $c=(6.4\pm 1.0)\times 10^{-6}$  M; and  $\psi_0=130\pm 20$  mV. The surface charge density was calculated from the surface potential using Eq. (2) to be  $\sigma_0=1e/(85\pm 20)$  nm $^2$ . These values are in agreement with earlier reports (Ref. 15). The inset shows the approach to contact over the final 50 nm in more detail. On the top left, a schematic of the force balance used here is shown.

have been described elsewhere.<sup>14,21</sup> Multiple beam interference allows the distance between the mica surfaces, which are silvered on their back sides, to be measured with resolution of  $\pm 0.2\text{--}0.3$  nm and their contact geometry (including  $R$ ) to be determined from the shape of the interference fringes.  $F$  is determined (to within  $\pm 100$  nN) directly from the bending  $\Delta D$  of the springs, as  $F=K_n\Delta D$ , where  $K_n=150$  N/m is the spring constant. After cleaning the apparatus and mounting the mica sheets, the surfaces are brought into contact in order to determine air-contact separation. The surfaces were then separated ( $\sim 2$  mm) and the cell in which they are mounted was filled with conductivity water, using a glass syringe. After allowing around 1–2 h for thermal equilibration, normal forces  $F(D)$  were measured as a function of the distance between the surfaces, at ambient room temperature ( $23\pm 1$  °C).

Purified (so-called conductivity) water was obtained by treating tap water with activated charcoal followed by a Millipore water purification system, consisting of RiOs™ and MILLI-Q® Gradient stage. The specific resistivity of the water, as produced within the purification system, was greater than  $18.2\text{ M}\Omega\text{cm}$ , which corresponds to an ion concentration of less than  $4\times 10^{-7}$  M for 1:1 salt concentration, and the total organic content was 4 ppb or less. In the cell the ion concentration (as deduced from the limiting Debye length)

was  $(6.4\pm 1)\times 10^{-6}$  M, attributed to the trace presence of ions described above. The  $pH$  value of the water prior to filling the apparatus was measured to be in the range 6.0–6.2 (due to dissolved  $\text{CO}_2$ ), and remained unchanged at the end of the experiments.

The mica used was ruby muscovite, grade 1, supplied by S & J Trading Inc., NY. Sym (diphenyl carbazide) (BDH analytical grade) or “EPON 1004F” resin (Shell) were used to glue the mica sheets to the cylindrical glass lenses. Results were the same (within scatter) for both glue types. The results shown in the figures are from four different experiments, and in one or two cases also from different contact positions between the mica surfaces within a given experiment.

## RESULTS

The normal force profiles  $F(D)$  vs.  $D$  from different experiments, measured during approach of the surfaces, are shown with the force axis is normalized as  $F(D)/R$ . Within the Derjaguin approximation (for  $R\gg D$ ),  $F(D)/2\pi R$  is the corresponding energy per unit area,  $E(D)$ , for two flat parallel surfaces a distance  $D$  apart,<sup>22</sup> making it possible to compare  $F(D)/R$  from different experiments. As a control prior to adding water, the jump-out distances and, from that, the interfacial energy were measured in air. We found a jump out distance of  $60\pm 10$  μm, corresponding to interfacial tension of  $-120\pm 15$  mN m $^{-1}$ , in agreement with earlier experiments for the case of unmatched mica sheets in air.<sup>23</sup> No significant difference was observed between consecutive jump-out from contact in air as a function of time.

$F(D)/R$  profiles measured during a first approach (or following a long equilibration period,  $>1$  h) are shown in Fig. 1. Long-ranged double-layer repulsive forces are observed due to the presence of a surface charge on the mica surfaces, which lose  $\text{K}^+$  ions to solution, and are due to the osmotic pressure of the counterions which are present in the gap between the surfaces to ensure overall charge compensation. The form of  $F(D)/R$  is well fitted by the DLVO model for a 1:1 electrolyte assuming constant surface potential,<sup>22</sup>

$$F/R = 128\pi ck_B T \kappa^{-1} \tanh^2(e\psi_0/4k_B T) \exp(-\kappa D) - A/6D^2, \quad (1)$$

where  $c$  is the ion concentration,  $T$  is the temperature,  $k_B$  is Boltzmann constant,  $A$  is the Hamaker constant of mica across water ( $2\times 10^{-20}$  J),  $\psi_0$  is the effective surface potential and  $\kappa^{-1}$  is the Debye length. The broken line in Fig. 1 (and in subsequent figures) was made using a fit to Eq. (1), which enables the decay length of the interactions and the effective surface charge to be extracted. Similarly good fits to our data are obtained using the nonlinear Poisson–Boltzmann equation<sup>24</sup> assuming constant surface charge density. There is no indication of hydration repulsion as would arise from trapping of hydrated  $\text{K}^+$  ions at the mica surfaces, and the surfaces come into a flat adhesive contact at  $D=D_0=0.0\pm 0.4$  nm (mica/mica contact, see Fig. 1 caption), in a single monotonic jump, from separations  $D=D_j=3.5\pm 1$  nm, in line with earlier observations.<sup>13,15</sup> The jump-in

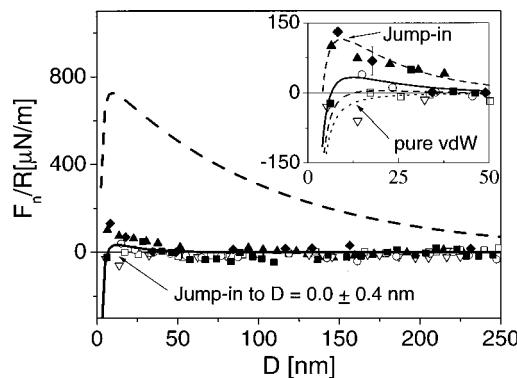


FIG. 2. Normal force-distance profiles (normalized by the radius of curvature) between curved mica surfaces in conductivity water [ $c = (6.4 \pm 1.0) \times 10^{-6}$  M,  $pH = 6.0-6.2$ ], measured  $5 \pm 2$  min after separation from contact (as in Fig. 1). Different symbols refer to different contact positions on different mica sheets. The broken line is the best fit of the DLVO expression, Eq. (1), with constant potential boundary condition, to the normal forces measured on first contact or following long equilibration (Fig. 1). The solid line (both in the main figure and in the inset) is the DLVO expression with  $\kappa^{-1} = 16 \pm 5$  nm and  $\psi_0 = 15 \pm 5$  mV. The inset shows the forces over the last 50 nm in more detail. The dashed lines at the inset correspond to the DLVO expressions with  $\kappa^{-1} = 19$  nm and  $\psi_0 = 24$  mV (upper line) and  $\kappa^{-1} = 15$  nm and  $\psi_0 = 11$  mV (lower line). The pure vdW attraction is shown as dotted line.

takes ca. 0.2–0.5 s. It is driven by the van der Waals (vdW) attraction between the surfaces overcoming the double-layer repulsion, and is a manifestation of the instability expected when the gradient of the force exceeds the normal spring constant of the spring attached to the lower lens (see the following section). On separation following the first adhesive contact (i.e., the first time the surfaces are brought into contact following their mounting in the SFB), significant jumps-out to  $D = 1.0 \pm 0.1 \mu\text{m}$  were observed. From the pull-off force  $F_p$  required to separate the surfaces, the solid–liquid surface tension  $\gamma = F_p/3\pi R$  was calculated to be  $-2.6 \pm 0.4 \text{ mN m}^{-1}$ . This value is slightly lower than earlier reports for conductivity water ( $\gamma = -3.9 \text{ mN m}^{-1}$ ).<sup>15</sup> The discrepancy may be due to the fact that mica from different sources has small natural variations in its composition, or possibly due to differing misalignment effects between the opposing mica surfaces.<sup>25</sup>

In order to test the reversibility of the measured forces, normal forces were measured during a subsequent approach within a time  $\tau = 5 \pm 2$  min after separation from contact. We note that  $\tau$  refers to the time when approach profiles start, and that it takes ca. 3 min to complete an  $F(D)$  versus  $D$  measurement (i.e., to go from  $D \sim 300$  nm down to contact). On this subsequent approach of the surfaces ( $\tau = 5 \pm 2$  min) the range of repulsive forces decreased dramatically as shown in Fig. 2, and jumps into a strong adhesive flat contact were observed already from  $D_j = 5.5 \pm 1$  nm. Such normal force measurements, taken following progressively longer waiting periods  $\tau = 10-50$  min after separation from contact, show a gradual increase in the long ranged repulsive force with increasing  $\tau$ , as shown in Fig. 3. After  $\tau$  of 1–2 h or longer, the normal forces were, within scatter, identical to their limiting long-time, i.e., equilibrium, behavior (see also force profile in Fig. 1 indicated with squares). The solid and

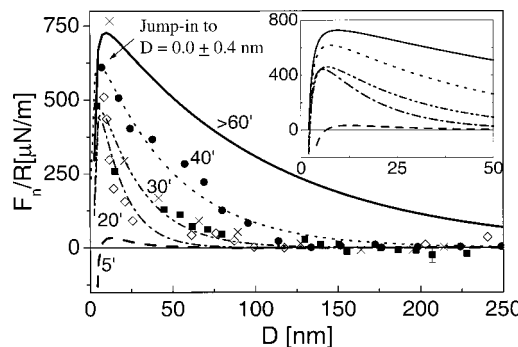


FIG. 3. Normal force–distance profiles between curved mica surfaces in conductivity water measured following different equilibration times  $\tau$  (values in minutes indicated next to the profiles) subsequent to separation from adhesive contact; the corresponding fits of the DLVO expression with constant potential boundary condition are shown as broken lines. The solid line is the best fit to the equilibrium normal forces (as Fig. 1). The 5'-dashed line is the fit to the forces measured on second compression and is taken from the main part of Fig. 2. The inset shows the best fits to the linear parts of the force profiles over the last 50 nm in more detail. The parameters of the fits are included in Table I.

broken curves in Fig. 3 are the fit of the data to the DLVO theory [Eq. (1)] for 1:1 salt solutions with constant potential boundary conditions (comparably good fits could be obtained with constant charge boundary conditions, see later in this work). The surface charge density,  $\sigma$ , was extracted from the profiles using the ion concentration,  $c$ , obtained from the Debye length,  $\kappa^{-1}$ , of the corresponding  $F(D)/R$  profile, and the standard relation<sup>22</sup>

$$\sigma = (8k_B T c \epsilon \epsilon_0)^{1/2} \sinh(e\psi_0/2k_B T). \quad (2)$$

The parameters of the DLVO fit (Debye length  $\kappa^{-1}$ , surface potential  $\psi_0$ , surface charge density  $\sigma$ , and ion concentration  $c$ ) are summarized in Table I and, in Fig. 4,  $\sigma$  and  $c$  are plotted as a function of  $\tau$ . We note that on separation from contact the jump-out distances were  $7 \pm 1 \mu\text{m}$ , corresponding to a  $\gamma = -15 \pm 3 \text{ mN m}^{-1}$ , in contrast to the much smaller values observed (above) for the jumps-out following the first time the surfaces came into contact. We remark on this later. The time over which the two surfaces remained in contact after jump-in varied from 1 to 12 min, although this did not influence the results.

TABLE I. Values of parameters used for best fit of the DLVO equation [Eq. (1), assuming constant potential] to the  $F(D)$  profiles for different compression runs.

$\tau$ (min)	$\kappa^{-1}$ (nm)	$c$ (mM)	$\psi_0$ (mV)	$\sigma$ ( $\text{mC m}^{-2}$ ) ( $\pm 0.1$ )
5 ± 2	15 ± 5	0.41 ± 0.18	11 ± 5	0.51
5 ± 2	16 ± 5	0.36 ± 0.15	15 ± 5	0.66
5 ± 2	19 ± 5	0.25 ± 0.08	24 ± 5	0.91
13 ± 3	15 ± 5	0.64 ± 0.11	23 ± 5	1.1
20 ± 3	15 ± 5	0.41 ± 0.17	39 ± 10	1.53
28 ± 3	30 ± 5	0.10 ± 0.04	60 ± 10	1.72
30 ± 3	25 ± 5	0.15 ± 0.06	48 ± 10	1.53
40 ± 3	45 ± 10	0.046 ± 0.022	76 ± 10	1.64
49 ± 3	40 ± 10	0.058 ± 0.03	76 ± 10	1.85
>60 ± 3	120 ± 20	0.0064 ± 0.0023	130 ± 20	1.85

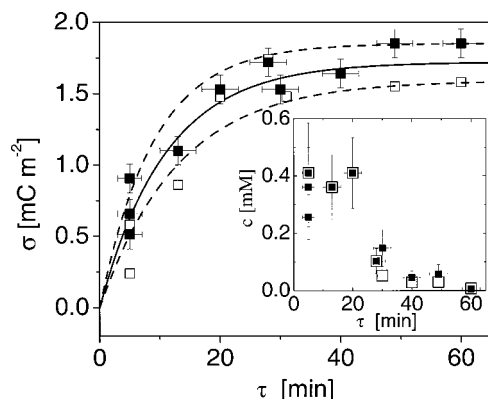


FIG. 4. The variation of the surface charge density  $\sigma$  with the equilibration time  $\tau$  following separation from contact, calculated according to the fit of the data to the DLVO theory with constant potential boundary conditions (solid symbols) (see Table I) and according to constant charge boundary conditions (Ref. 24) (open symbols). The solid line is the best fit of the data to an exponential growth of the form:  $\sigma(\tau) = \sigma_0[1 - \exp(-\tau/\tau_r)]$ , with a time constant  $\tau_r = 11$  min and  $\sigma_0 = 1.72 \text{ mC m}^{-2}$ . The broken lines are similar functions with  $\tau_r = 13$  min and  $\sigma_0 = 1.6 \text{ mC m}^{-2}$  (lower line) and  $\tau_r = 9$  min and  $\sigma_0 = 1.85 \text{ mC m}^{-2}$  (upper line). The inset shows the variation of the ion concentration  $c$  (obtained from the fitted Debye lengths) with  $\tau$ . The symbols correspond to those in the main figure.

## DISCUSSION

Our main finding is that following the approach into adhesive contact across conductivity water, mica surfaces that are then separated regain their characteristic surface charge density only slowly, over time scales of around an hour for full equilibrium (it is of interest that this time is consistent with the slow  $\text{H}^+/\text{Li}^+$  ion exchange process on Li-treated delaminated mica).<sup>12</sup> To understand this quantitatively it will be helpful to review briefly the state of mica surfaces in aqueous media.

The surface of cleaved mica is covered with  $\text{K}^+$  ions (with an area per site of  $0.48 \text{ nm}^2$ ) and in air the surface is overall electrically neutral. When immersed in conductivity water, the  $\text{K}^+$  ions are dissolved, due to an ion exchange process at the surface (intracrystalline exchange does not occur).<sup>11</sup> At the  $pH \sim 6$  and very low ion concentrations of our experiments, most of the  $\text{K}^+$  ions are effectively exchanged with  $\text{H}_3\text{O}^+$  ions, which are at a higher concentration.<sup>11,15</sup> In equilibrium, it is thermodynamically favorable for the surface associated positive counterions ( $\text{K}^+$  or  $\text{H}_3\text{O}^+$  ions) to be in the solution as the free energy gain due to translational entropy exceeds the ionization enthalpy at the relevant surface lattice sites. On approach of the surfaces, once the distance between them is small enough, the entropy gained by being in solution (in the intersurface gap) becomes sufficiently small that the positive counterions—predominantly  $\text{H}_3\text{O}^+$  in our case—condense back into the surface,<sup>26</sup> neutralizing it. The combination of the mica crystal structure,<sup>27</sup> together with the relatively detachable hydration sheath about them,<sup>15,18</sup> allows the protons to condense readily into the mica/mica lattice sites. Van der Waals attraction then dominates the forces between the surfaces, and they come into strong adhesive molecular contact.

On separation of the surfaces, conductivity water is sucked back into the gap between them, and the initially

neutral surfaces find themselves out of equilibrium. The ions from the ionizable surface sites are then gradually released back into the solution, rebuilding the surface charge density within an hour or more. Because the ionization process is slow, immediately following decompression the surface charge  $\sigma$  is momentarily very small; thus only a weak double layer repulsive force is measured immediately after separation, increasing at longer  $\tau$  until equilibrium is established.

The slowness of attainment of equilibrium suggests that in the case of conductivity water, following first compression, there is a substantial energy barrier opposing the return of the surface ions into the water.<sup>28</sup> We can try to estimate this barrier from the variation of the surface charge density with the time,  $\tau$ , between first and second compression, as plotted in Fig. 4. The solid line is the best fit of the data to an exponential growth of the form:

$$\sigma(\tau) = \sigma_0[1 - \exp(-\tau/\tau_r)], \quad (3)$$

from which a characteristic time,  $\tau_r = 11 \pm 2$  min, is obtained, where  $\sigma_0 = 1.72 \pm 0.13 \text{ mC m}^{-2}$  is the surface charge density at equilibrium (Fig. 1).

Setting  $\tau_r^{-1} = A_0 \exp(-E_a/k_B T)$ , assuming an Arrhenius constant  $A_0$  (effectively a microscopic jump frequency) in the range  $10^{10}\text{--}10^{13} \text{ s}^{-1}$ ,<sup>29</sup> an activation energy  $E_a = 83 \pm 10 \text{ KJ mole}^{-1}$  ( $33 \pm 4 k_B T$ , for  $T = 298 \text{ K}$ ) for the release of the ions from the mica surface into the water is obtained. The  $\text{OH}^-$  groups are located inside the mica surface and the radius of the potassium lattice site,  $r_0$ , is  $0.14 \text{ nm}$ .<sup>27,30</sup> When the ions are within the mica surface, the  $\text{OH}^-$  groups stabilize their high self-energy. In water this energy is reduced due to the high dielectric constant of the medium. However, we find that the transfer from the surface to the water involves a high energy barrier, which must be related to the high self-energy of the ion in the transition state. One would expect the varying local modification of water structure in the hydration shell of the ions as they transfer from the mica to the water to contribute significantly to the activation barrier. Indeed the energy barrier we find is similar to the dehydration energy required to remove (to infinity) one or two water molecules out of the hydration shell of a monovalent cation.<sup>31</sup>

It is appropriate to comment on the magnitude and variation with time of the effective ion concentration  $c$  extracted from the  $F(D)$  profiles, as appears in Table I and in the inset to Fig. 4. This appears to be at higher values for  $t$  in the range 5–20 min before decreasing to the bulk value for conductivity water at large  $\tau$ . The reason for this, we believe, is qualitatively as follows: Following the adhesive contact between the mica sheets and their subsequent separation, ions from the surfaces begin to be released into the conductivity water (at its bulk concentration) that is sucked into the intersurface gap. After a time  $\tau$  the surface charge concentration has increased to  $\sigma(\tau)$ , and during the approach—as  $F(D)$  is being measured—more ions are released. The precise balance between the ion release, their diffusion across the gap and laterally out of it, and the squeezing out of ions as the surfaces approach is difficult to analyze quantitatively. If we assume that the ions being released over a period of, say,  $\tau_r$ —the time of measurement—remain within a gap of di-

mension  $D'$ , we may then roughly estimate their expected concentration within the gap. The net surface charge will be increased in that time from  $\sigma(\tau)$  to  $\sigma(\tau+t_r)$ , given by Eq. (3). The mean ion concentration  $c'$  in the gap will then be  $c' = 2\delta\sigma/D'e$ , where  $e$  is the electronic charge ( $1.6 \times 10^{-19}$  C) and  $\delta\sigma = \sigma(\tau+t_r) - \sigma(\tau)$ . Putting  $D' = 25$  nm as a typical value and using Eq. (3) with  $\sigma_0 = 1.7 \text{ mCm}^{-2}$  gives  $c \approx 0.2 \text{ mM}$  for  $\tau = 5$  min. This is comparable to the initial values of the effective ion concentration in the gap, which are in the range ca.  $0.15$ – $0.5$  mM (inset to Fig. 4).

In the absence of electrostatic repulsion the mica surfaces are expected to attract each other more strongly when close to contact, increasing the jump-in distance as they approach. We can estimate the extent of this effect more quantitatively, as follows. The jump-in is expected when  $\partial F/\partial D > K_n$ , the spring constant. A good estimate for the attractive force is given by the theoretical vdW force expected between two crossed cylinders of radius of curvature  $R$ , at closest distance  $D$ ,  $F(D) = -AR/6D^2$ , where  $A$  is the Hamaker constant of two mica surfaces separated by water ( $A = 2 \times 10^{-20}$  J). The condition for a jump-in is thus:  $\partial F/\partial D = AR/3D^3 > K_n = 150 \text{ N/m}$ , from which we obtain the maximum distance  $D_j$ , from which a jump-in can occur to be  $D_j < (AR/3K_n)^{1/3} = 6$  to  $7.6$  nm, for  $R = 0.5$  to  $1$  cm. The jump-in observed on first approach or following equilibration (large  $\tau$ ) was from distances of  $3.5 \pm 1$  nm, because in addition to vdW attractive force there was a repulsive double layer force, which decreases the distance from which the jump-in occurs. On second compression, the double layer repulsive force was much weaker, and a jump-in from distances of  $5.5 \pm 1$  nm is observed, quite comparable to the expected value for the case of pure vdW attraction (6–7.6 nm). Concerning the magnitude of the adhesion, Lifshitz theory predicts the adhesion energy  $E_0$  expected from the vdW forces to be  $E_0 = 2\gamma = -A/12\pi D_s^2 = F/2\pi R$ , where  $D_s$  is an effective cutoff separation when the two surfaces are in contact (typical values are  $0.16$ – $0.2$  nm<sup>25</sup>). For water, putting  $D_s = 0.18$  nm gives  $E_0 = 16 \text{ mN/m}$ , similar to the values measured on pulloff from adhesive contact subsequent to the first approach, suggesting that the adhesion energy is mainly determined by the vdW forces. The much lower effective surface energy (ca.  $2.6$  mN/m) consistently measured from the pulloff force following the *first* time the surfaces come into contact is intriguing. We do not have an unambiguous explanation for this, though it may be due to local rearrangement within the near-surface region of the mica, or possibly to a slight mutual shift of the surface layers into a more favorable registry on first contact and separation.

## CONCLUSIONS

The time dependence of the normal forces between two mica surfaces immersed in conductivity water were studied. On first approach to contact (assumed to be characteristic of equilibrium conditions) the counterions are forced back into the mica surfaces; immediately following separation of the surfaces the long-ranged repulsive double layer forces are reduced markedly relative to those observed on first approach, due to transient reduction of the surface charge. With time there is a slow release of counterions from the mica

surfaces into the water, resulting in a slow relaxation of normal forces to their equilibrium values. From the rate at which equilibrium is attained an effective activation energy of ca.  $33 k_B T$  for the ion release may be estimated, in reasonable agreement with what is expected from binding of ions to the mica surface lattice.

## ACKNOWLEDGMENTS

The authors thank Nir Kampf for his help, and Phil Pincus, Jacob Israelachvili, Sam Safran, Tom Witten, Dima Lukatsky, and Anton Zilman for useful discussions. The US–Israel Binational Science Foundation, the Deutsche–Israel Program (DIP), and the Minerva Foundation are thanked for their support. U.R. thanks the Eshkol Foundation for a studentship.

- <sup>1</sup>M. C. Bellissent-Funel, J. Lal, and L. Bosio, *J. Chem. Phys.* **98**, 4246 (1993).
- <sup>2</sup>M.-C. Bellissent-Funel, S. H. Chen, and J. M. Zanotti, *Phys. Rev. E* **51**, 4558 (1995).
- <sup>3</sup>S.-H. Chen and M.-C. Bellissent-Funel, in *Hydrogen Bond Networks*, edited by M.-C. Bellissent-Funel and J. C. Dore (Kluwer Academic, Dordrecht, 1994), Vol. 435, pp. 307–336.
- <sup>4</sup>J. Clifford, in *Water in Disperse Systems*, edited by F. Franks (Plenum, New York, 1975), Vol. 5, pp. 75–132.
- <sup>5</sup>P. Pissis, J. Laudat, D. Daoukaki-Diamanti, and A. Kyritsis, in *Hydrogen Bond Networks*, edited by M.-C. Bellissent-Funel and J. C. Dore (Kluwer Academic, Dordrecht, 1994), Vol. 435, pp. 425–432.
- <sup>6</sup>M. A. Ricci, F. Bruni, P. Gallo, M. Rovere, and A. K. Soper, *J. Phys.: Condens. Matter* **12**, A345 (2000).
- <sup>7</sup>P. J. Rossky, in *Hydrogen Bond Networks*, edited by M.-C. Bellissent-Funel and J. C. Dore (Kluwer Academic, Dordrecht, 1994), Vol. 435, pp. 337–338.
- <sup>8</sup>F. Bruni, M. A. Ricci, and A. K. Soper, *J. Chem. Phys.* **109**, 1478 (1998).
- <sup>9</sup>J. N. Israelachvili and H. Wennerstrom, *Nature (London)* **379**, 219 (1996).
- <sup>10</sup>J. P. Quirk, *Isr. J. Chem.* **6**, 213 (1968).
- <sup>11</sup>G. L. Gaines, *J. Phys. Chem.* **61**, 1408 (1957).
- <sup>12</sup>M. A. Osman, W. R. Caseri, and U. W. Suter, *J. Colloid Interface Sci.* **198**, 157 (1998).
- <sup>13</sup>J. N. Israelachvili and G. E. Adams, *J. Chem. Soc., Faraday Trans. 1* **79**, 975 (1978).
- <sup>14</sup>J. Klein, *J. Chem. Soc., Faraday Trans. 1* **79**, 99 (1983).
- <sup>15</sup>R. M. Pashley, *J. Colloid Interface Sci.* **80**, 153 (1981).
- <sup>16</sup>U. Raviv, P. Laurat, and J. Klein, *Nature (London)* **413**, 51 (2001).
- <sup>17</sup>V. A. Parsegian, *Adv. Colloid Interface Sci.* **16**, 49 (1982).
- <sup>18</sup>R. M. Pashley, *J. Colloid Interface Sci.* **83**, 531 (1981).
- <sup>19</sup>R. M. Pashley and J. N. Israelachvili, *J. Colloid Interface Sci.* **101**, 511 (1984).
- <sup>20</sup>One or two cases of hysteretic behavior of the forces between mica surfaces across aqueous salt solutions have been reported, e.g., in Ref. 13, Fig. 9, and in C. Toprakcioglu, J. Klein and P. F. Luckham, *J. Chem. Soc., Faraday Trans. 1* **83**, 1703 (1987), and may have been due to transient presence of surfactants on the mica surfaces.
- <sup>21</sup>J. Klein and E. Kumacheva, *J. Chem. Phys.* **108**, 6996 (1998).
- <sup>22</sup>B. V. Derjaguin, N. V. Churaev, and V. M. Muller, *Surface Forces* (Plenum, New York, 1987).
- <sup>23</sup>A. I. Bailey and S. M. Kay, *Proc. R. Soc. London, Ser. A* **301**, 47 (1967).
- <sup>24</sup>D. Y. C. Chan, R. M. Pashley, and L. R. White, *J. Colloid Interface Sci.* **77**, 283 (1980).
- <sup>25</sup>P. M. McGuigan and J. N. Israelachvili, *J. Mater. Res.* **5**, 2232 (1990).
- <sup>26</sup>I. Rouzina and V. A. Bloomfield, *J. Phys. Chem.* **100**, 9977 (1996); P. Pincus (private communication).
- <sup>27</sup>W. L. Bragg, *Atomic Structure of Minerals* (Cornell University Press, Ithaca, 1937), pp. 203–216; G. L. Gaines and D. Tabor, *Nature (London)* **178**, 1304 (1956).
- <sup>28</sup>It is noteworthy that, in contrast to the present results in conductivity water, there appears to be little hysteresis in the surface forces for the case of added salt where the salt concentration is sufficiently low that the surfaces jump into contact on approach. Both earlier reports (for the case of  $10^{-4}$  M  $\text{KNO}_3$ , Ref. 13), and experiments by us (for the case of

$10^{-3}$  M NaCl, to be published) found no significant relaxation or time dependence of the normal forces. This may be due to the effect of co-ions near the surfaces in reducing the effective activation energy for ion release from the mica lattice.

<sup>29</sup> W. J. Moore, *Physical Chemistry*, 5th ed. (Longman Scientific & Technical, London, 1972).

<sup>30</sup> Although the detailed microscopic structure and ionisation processes are complicated and it is probably not valid to use the concept of bulk dielectric constants, it is of interest to estimate the effective values of these if the positively charged ions condensed to a distance  $r_0$  from the  $\text{OH}^-$  groups. Assuming that the electrostatic interaction energy to remove the protons from the lattice may be identified with the activation energy  $E_a$ , the effective dielectric constant  $\epsilon_{\text{eff}}$  for the interaction is then  $\epsilon_{\text{eff}} = e^2/4\pi\epsilon_0 r_0 E_a = 12 \pm 2$ . This is somewhat higher than the dielectric con-

stant of mica ( $\sim 5-7$ ) and much less than that of water (80.1): Since on detaching the proton from the  $\text{OH}^-$  it will initially be in a mica environment, and subsequently in a water environment, this value for  $\epsilon_{\text{eff}}$  (bearing in mind our reservations concerning the use of such bulk parameters for these microscopic processes) therefore seems not unreasonable. Arrangement of water molecules about the ions must contribute to the activation energy and cannot be neglected; nonetheless this naive calculation is of interest in indicating that the mean value of the net effects is somewhere between what would be expected for pure water and for bulk mica.

<sup>31</sup> P. P. S. Saluja, in *Electrochemistry*, edited by J. O. M. Bockris (Butterworths, London, 1976), Vol. 6, pp. 2-51.

<sup>32</sup> H. Poppa and A. G. Elliot, *Surf. Sci.* **24**, 149 (1971).

<sup>33</sup> D. Tabor and R. H. Winterton, *Proc. R. Soc. London, Ser. A* **312**, 435 (1969).